Characterization of enhanced $D\alpha$ high-confinement modes in Alcator *C*-Mod*

M. Greenwald,† R. Boivin, P. Bonoli, R. Budny,[a] C. Fiore, J. Goetz, R. Granetz, A. Hubbard, I. Hutchinson, J. Irby, B. LaBombard, Y. Lin, B. Lipschultz, E. Marmar, A. Mazurenko, D. Mossessian, T. Sunn Pedersen, C. S. Pitcher, M. Porkolab, J. Rice, W. Rowan,[b] J. Snipes, G. Schilling,[a] Y. Takase,[c] J. Terry, S. Wolfe, J. Weaver,[d] B. Welch,[d] and S. Wukitch
MIT-Plasma Science and Fusion Center, Cambridge, Massachusetts 02139

(Received 16 November 1998; accepted 21 January 1999)

Regimes of high-confinement mode have been studied in the Alcator *C*-Mod tokamak [Hutchinson *et al.*, Phys. Plasmas **1**, 1511 (1994)]. Plasmas with no edge localized modes (ELM-free) have been compared in detail to a new regime, enhanced $D\alpha$ (EDA). EDA discharges have only slightly lower energy confinement than comparable ELM-free ones, but show markedly reduced impurity confinement. Thus EDA discharges do not accumulate impurities and typically have a lower fraction of radiated power. The edge gradients in EDA seem to be relaxed by a continuous process rather than an intermittent one as is the case for standard ELMy discharges and thus do not present the first wall with large periodic heat loads. This process is probably related to fluctuations seen in the plasma edge. EDA plasmas are more likely at low plasma current ($q>3.7$), for moderate plasma shaping, (triangularity ~ 0.35–0.55), and for high neutral pressures. As observed in soft x-ray emission, the pedestal width is found to scale with the same parameters that determine the EDA/ELM-free boundary. © *1999 American Institute of Physics.* [S1070-664X(99)94605-0]

I. BACKGROUND

Alcator *C*-Mod is a compact (major radius $R=0.67\,\mathrm{m}$, minor radius $a=0.22\,\mathrm{m}$), high field tokamak ($2.6<B_T<7.9\,\mathrm{T}$), which operates with plasma currents between 0.23 and 1.5 MA and average electron densities between 0.24 and $5.9\times10^{20}\,\mathrm{m}^3$ (gas fueled). The standard configuration for *C*-Mod plasmas is with a lower single null and a tightly closed divertor. Normal operation is with the ∇B ion drifts toward the *x* point. Plasma facing components are made of molybdenum and are coated with boron roughly twice a month during each campaign. In the standard divertor configuration, *C*-Mod has an elongation (κ) between 1.55 and 1.75, lower triangularity (δ_L) near 0.55, and an upper triangularity (δ_U) near 0.3. Up to 3.5 MW of ion cyclotron range of frequencies (ICRF) power at 80 MHz is available, from two dipole antennas, each with 0, π phasing; the cases described here are all with *H* minority heating. Total input power can reach 4.5 MW.

II. ENHANCED $D\alpha$ (EDA) AND EDGE LOCALIZED MODE-FREE (ELM-FREE) H-MODES

The ELMy (high-confinement mode) H Mode is the only enhanced confinement mode which has previously demonstrated steady-state potential. However, the peak heat loads associated with type I ELMs can reach unacceptable levels when extrapolated to reactor scale devices. Attempts to limit the loss per ELM in joint European Torus (JET) resulted in severe degradation of energy confinement.[1] In Alcator *C*-Mod, we have studied a promising H-mode regime,[2,3] which is characterized by good energy confinement, moderate particle confinement, and no large, type I ELMs.[4] (See Ref. 4 for a more complete description of ELM types.) The pedestal electron temperature can reach 600–800 eV, well above the measured threshold for type III ELMs, and the pressure gradient in the transport barrier is near or above first regime magnetohydrodynamic (MHD) stability limits. While the ion temperature is not measured in the pedestal, at the high densities that exist in *C*-Mod, these must be within 50–100 eV of the electrons to satisfy conservation of energy. We have named this regime EDA or enhanced D_α H mode after its salient characteristic. Figure 1 shows a set of traces comparing typical ELM-free and EDA discharges. The ELM-free discharge shown accumulates impurities and ends in a radiative collapse. The ratio of radiated power to plasma density, P_{RAD}/n_e, which is an indication of the impurity density, rises by a factor of 4. In most such discharges the high radiation phase is followed by a back transition to low-confinement mode (L mode). In contrast, the EDA can last, without obvious change, for the duration of the radio-frequency (rf) heating pulse, about 10 energy confinement times. Unlike standard ELMy discharges, which undergo periodic relaxation oscillations, EDA plasmas show no significant intermittent loss of energy and particles. The edge gradients seem to be limited by a continuous process

The lack of impurity accumulation in EDA does not, by

*Paper B1I1.3 Bull. Am. Phys. Soc. **43**, 1636 (1998).
†Invited speaker.
[a]Princeton Plasma Physics Lab, Princeton, New Jersey.
[b]Fusion Research Center, University of Texas, Austin, Texas.
[c]Department of Physics, University of Tokyo, Japan.
[d]University of Maryland, College Park, Maryland.

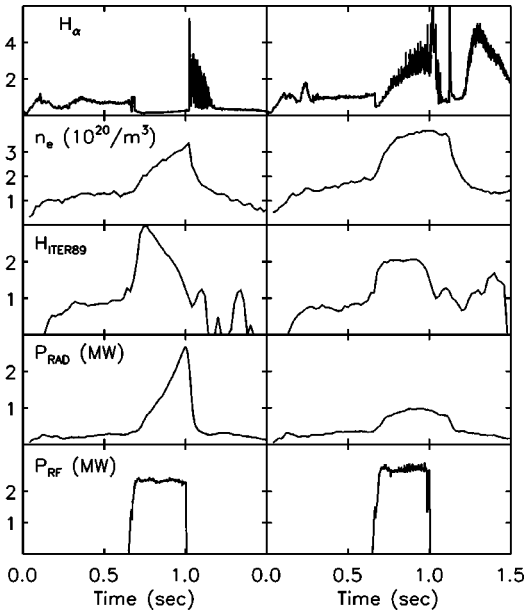

FIG. 1. Characteristic traces from ELM-free and EDA H modes. Note the difference in the H α and P_{RAD} signals. The controlling difference between these shots is the target density, which is higher for EDA.

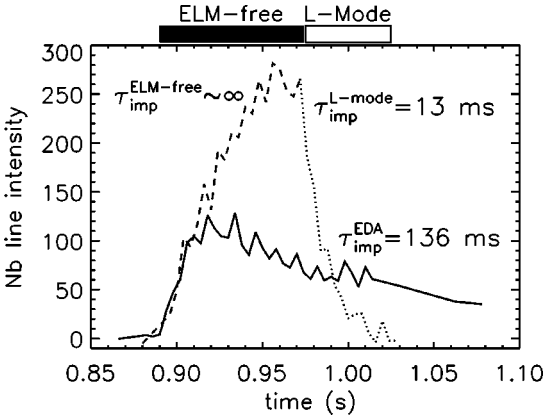

FIG. 2. A comparison of impurity confinement for ELM-free and EDA H modes from laser blow-off experiments. No loss of impurities is seen during the ELM-free phase seen in the upper trace. When this discharge transitions back to L mode, the impurities are lost rapidly. The lower trace is for an otherwise similar EDA discharge. In this case the global impurity confinement is about twice the energy confinement time.

itself, constitute proof of lower particle confinement. For intrinsic impurities, the source rate, which is highly nonuniform and quite difficult to measure, may be varying as well. To clarify this point, nonintrinsic, nonrecycling impurities were injected by laser blow-off into the various types of discharges.[5] The result of such an experiment can be seen in Fig. 2. In this case, the injected impurity was niobium whose sodiumlike state was observed with an extreme ultra-violet (XUV) spectrometer. This ionization state predominates in regions of the plasma where $T_e \sim 900-1200$ eV, that is, inside the pedestal region. Modeling of its atomic physics using measured plasma profiles and comparisons with soft x-ray spectra of higher ionization states show that the strength of lines from this species provides a reasonably good representation of the total niobium inventory. For ELM-free H modes, no decay of the niobium signal can be seen. The gradual rise in the signal is likely due to internal rearrangement of the niobium charge states. At about 0.97 s, the discharge drops back into L mode during which the niobium decay is rapid. In the same figure, an example of impurity injection into an EDA H mode is shown. In this case the particle confinement time is 0.136 s, about twice the global energy confinement time. Detailed studies of impurity profile evolution have shown that the change in particle transport occurs in a relatively narrow region at the plasma edge.[5]

EDA may be related to regimes seen on other devices. JET has reported low particle confinement (LPC) H-modes[6] which, like EDA, were obtained with ICRF heating. These plasmas were double null with triangularity in the range of 0.3–0.5, shapes that have not been possible more recently in JET since the installation of divertor hardware. EDA also shares some characteristics with the small ELM behavior seen on (JAERI tokamak) JT60-U when the plasma triangularity was increased[7] and also to the type II ELMy regime reported by DIII-D.[8] The LPC mode lasted only about 1 s. Type II ELMy discharges were also transient, with type I ELMs eventually returning in all cases. These regimes share with EDA the characteristics of finite impurity confinement with benign or missing ELMs. The occurrence of these regimes is consistent with the effects of plasma shaping which are described in more detail below; the disappearance of large ELMs is strongly correlated with plasma triangularity.

The connection between EDA and other ''small'' ELM regimes is made somewhat confusing by the appearance of low amplitude ELMs on top of the EDA background. Shown in Fig. 3, these ELMs are seen when β rises above a level approximately characterized by $\beta_N \sim 1.2-1.3$. If this behavior were common to other devices, which typically run at lower field and thus higher β, they might never see a ''pure'' EDA. As seen on $H\alpha$, these ELMs have a bipolar character, with a rapid excursion below the EDA background level preceding the positive signal. The ELMs can also be seen in the ion saturation currents of langmuir probes mounted in divertor tiles, demonstrating that some particle loss is associated with each ELM. However, no corresponding particle or energy loss from the core plasma can be seen on the line averaged density or in the diamagnetic stored energy. The measurement of these quantities has a signal to noise ratio over 200 implying that core losses would be less than 0.5% per ELM in this regime. This should be compared to 2%–10% losses measured for type I ELMs.[4] These small ELMs are observed with a soft x-ray array as very small perturbations near the base of the pedestal. Correlation analysis of the magnetic signatures of these ELMs shows that the magnetic perturbations are counter-rotating at poloidal velocities equivalent to ~25 km/s, typical of edge values in H-mode. The signal coherence is rather low, the modes growing quickly and lasting not much more than one cycle. The power spectrum is broad and noisy. In so far as there is a dominant mode it is $n \sim 1$, $m \sim 4-5$, resonant with the edge q and at a frequency near 30 kHz with the magnetic signals stronger on the high-field side. No ballooning precursors are observed, unlike type III ELMs which occur at much lower

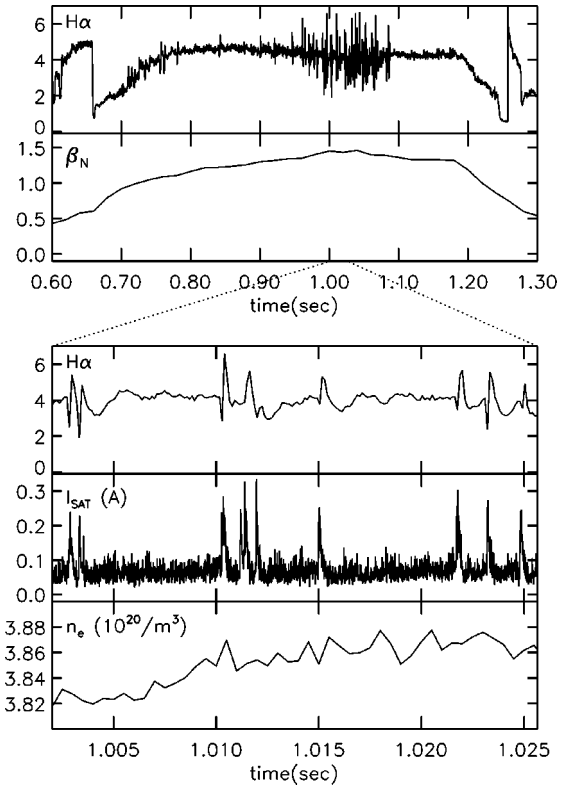

FIG. 3. As β_N rises above 1.2–1.3 small ELMs appear on top of the EDA. Also shown on an expanded time scale is $H\alpha$, the ion saturation current from a divertor probe and the line averaged density. While some plasma exhaust is clearly visible on the probes, there is no measurable loss of particles from the core plasma.

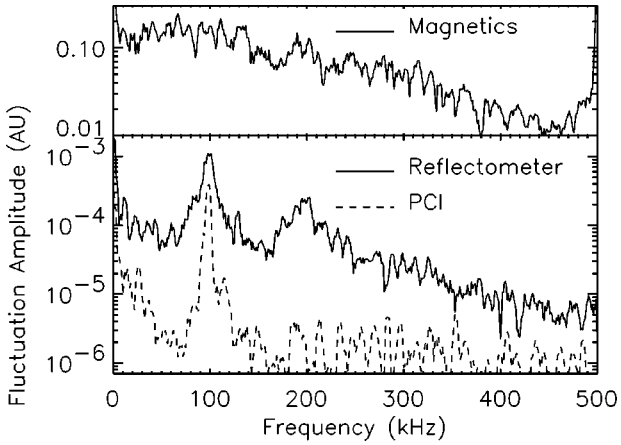

FIG. 4. Power spectra for fluctuations seen during EDA. The reflectometer sees broadband turbulence with a quasicoherent feature superimposed. With phase contrast imaging (PCI), only the coherent feature is observed; k_R is found to be in the range of 2–5 cm^{-1}. Fast magnetic probes see only the broadband fluctuations. The differences are probably due to the different views and k resolution of the diagnostics. The reflectometer measurement is well localized radially near the foot of the pedestal. The PCI is a line integral measurement through the entire plasma cross section. The magnetics would not be very sensitive to short wavelength modes.

edge temperatures and pressures.[9] Overall, the magnetic signature seems closer to that of type I ELMs.[4]

Global energy confinement for EDA plasmas is about 15% higher than the (International Thermonuclear Experimental Reactor) ITER97y H-mode scaling derived for ELMy plasmas.[10] Energy confinement enhancement relative to the ITER89 L-mode scaling[11] is found to be, on average, 1.9 for EDA discharges and 2.1 for ELM-free. The difference in confinement between the two regimes reflects the difference in the magnitude of their pedestal temperatures. Note that there is no discernable difference in the core density or temperature profile shapes between EDA and ELM-free H modes. The characterization of these profiles and their significance for transport is detailed in Ref. 3. In *C*-Mod, a simple offset-linear relation exists between edge temperature and global confinement.[3] This relation is consistent with marginal stability and critical gradient-length models of plasma transport. As a result, anything that depresses the edge temperature will also degrade energy confinement. For example, high neutral pressures are associated with lower confinement. Plasmas with midplane pressures greater than 0.2–0.3 mTorr (divertor pressures $>$40 mTorr) begin to show a drop in confinement, a trend which continues to the highest recorded pressures which were above 1 mTorr (divertor pressure $\sim$150–200 mTorr) where τ_E is close to L-mode levels. The drop in confinement is continuous and even in the extreme cases, the discharges are clearly still in H mode; discrete transitions can be seen on edge diagnostics when the plasma returns to L mode. For discharges with power radiated from inside the last closed flux surface higher than 50% of the input power, confinement also begins to decrease, reaching L-mode levels for radiated fractions over 0.9.[3] When comparing with global scaling laws, consideration is limited to discharges with radiated power fraction $<$0.50 and divertor neutral pressure $<$40 mTorr.

The difference in pedestal temperature and impurity confinement in EDA may be the result of transport driven by enhanced levels of turbulence which have been observed in the edge of these plasmas. The EDA is characterized by much higher levels of density fluctuations which are seen by phase contrast imaging (PCI) and reflectometry.[12,13] The fluctuations seen by the reflectometer are broadband, extending to at least 400 kHz and are usually accompanied by a quasicoherent feature which can appear anywhere from 60 to 130 kHz. The reflectometer views a small region of plasma at the outer midplane, typically near the foot of the pedestal in H mode. The PCI diagnostic consists of a set of closely spaced channels viewing vertically through the plasma cross section. It is sensitive to the k_R component of density fluctuations in the range of 1–5 cm^{-1}. As seen in Fig. 4, the PCI sees mainly the quasicoherent feature. If we assume that these two diagnostics are measuring the same edge-localized fluctuation, then the k_R of the PCI is equivalent to k_θ. The frequency of the coherent component is correlated with the $H\alpha$ level and is modulated by about 10%–20% at the sawtooth period. Unlike the $H\alpha$ signal, which may suggest that the ELM-free to EDA transition is gradual, the density fluctuations are seen to turn on abruptly. When plasma parameters are slowly varied to explore the EDA/ELM-free boundary (see Sec. III and Fig. 6 below), there is evidence, on the $H\alpha$ signal, of ''dithers'' between the two regimes. EDA is also accompanied by higher levels of magnetic fluctuations.[9,14] These are also broadband, extending at least

to several hundred kHz and without any discernable coherent component (Fig. 4). The lack of this feature, which is observed at 2–5 cm^{-1} with PCI, may be due to the magnetics diagnostic's lack of sensitivity of very short wavelength modes. The magnetic fluctuations are seen to rotate rapidly in the electron diamagnetic direction, an observation consistent with the presence of a strong negative radial electric field in the plasma edge. Perpendicular rotation speeds are typically in the range of 20–60 km/s implying radial electric field magnitudes of 100–250 kV/m.

III. EDA AND ELM-FREE H-MODE OPERATIONAL SPACE

A series of experiments was undertaken to study the conditions under which either ELM-free or EDA H modes are obtained. These studies involved scans of magnetic field, plasma current, density, heating power, and triangularity. In analyzing the results of these experiments it was necessary to define a quantitative metric for sorting discharges into one or the other regime. While most H-mode plasmas are clearly classified as one or the other, a certain amount of ambiguity exists in some cases. The D_α level itself is probably not the best measure, particularly for transient conditions. This is not surprising considering the geometric distribution of this light and its origin as part of both ionization and recombination processes. The presence of high frequency edge fluctuations may be the best indicator, but these observations were not available for all times or for all discharges. As a practical matter, we chose to use impurity accumulation as the final arbiter. Plasmas with impurity radiation steadily increasing with a time constant less than 0.5 s (and, of course, with no ELMs) were classified as ELM-free.

Operation at higher plasma currents usually results in ELM-free plasmas. Figure 5(a) shows the results of an I_P scan. For the standard shape, and $B_T = 5.4$ T a transition occurs near 1 MA, and EDA discharges are generally absent at 1.2 MA and above. Under the conditions of this scan, 1 MA corresponds to q at the 95% flux surface, $q_{95} = 3.7-4.0$. Magnetic field scans at constant current of 1 MA [Fig. 5(b)], show a transition to EDA as q_{95} rises to near 4. We can see from the figure that the transition to EDA occurs at approximately the same q_{95} in both cases. Plasma shape also seems to play an important role in determining the type of H mode. For otherwise identical conditions, discharges with the lowest and highest δ were consistently ELM-free while those with moderate δ were more likely to be EDA. (Both δ_L and δ_U were scanned, at times separately and in other cases simultaneously. So far, the trends reported here are not clearer when plotted against the separate quantities so we have chosen to characterize the shaping by their average value.) Similar trends can be observed clearly, in individual discharges where δ is scanned dynamically as shown in Fig. 6. The effect of shaping cannot be explained simply as the variation in q_{95} at constant current. In fact, the trends can be opposite to those described above. Figure 5(c) shows the two regimes in the δ, q_{95} plane. In this case, discharges at higher q are ELM-free. Thus we must conclude that the EDA/ELM-free boundary depends on both q_{95} and shape. It should be noted

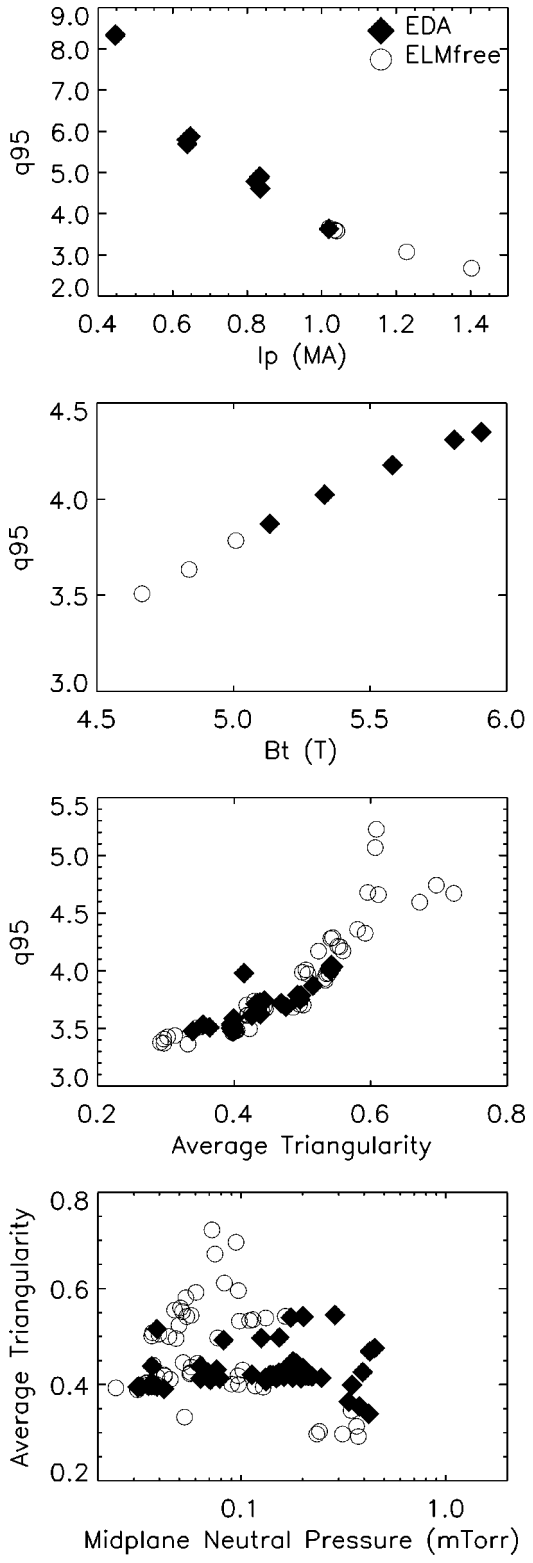

FIG. 5. Results of studies to determine EDA-ELM-free boundary. (a) Plasma current scan at 5.3 T and standard *C*-Mod plasma shape. The transition occurs at about 1 MA or $q_{95} \sim 3.8$. (b) A magnetic field scan at $lp = 1$ MA and standard shape. Again the transition occurs at $q_{95} \sim 3.8$. (c) q_{95} plotted for data from triangularity scan. In this case ELM-free discharges occur at both the highest and lowest values of q_{95}, suggesting a dependence on both shape and safety factor. (d) Occurrence of the two regimes as a function of average triangularity and midplane neutral pressure. EDA discharges are seen to occur at moderate values of triangularity and are more likely at higher neutral pressure.

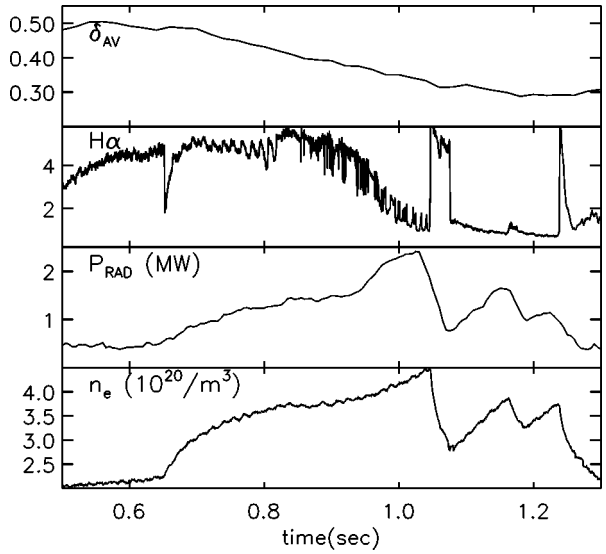

FIG. 6. Time histories of several plasma parameters during a continuous scan of both upper and lower triangularity (δ). As δ falls below 0.35, the plasma makes a transition from EDA to ELM-free. This is clearly visible in the $H\alpha$ signal and also from the increase in particle confinement evidenced by the radiated power and density. The fluctuations in the $H\alpha$ signal during the transition are not the ELMs discussed above, but may be ''dithers'' between the two H-mode regimes.

that changes in plasma triangularity can effect the coupling to the divertor; thus shaping effects cannot be entirely isolated. If this effect is important it would not be related to the scrape-off layer (SOL) connection length which is essentially constant for the δ scan, but could be related to changes in neutral dynamics and recycling. EDA plasmas are more likely at the highest target plasma densities and high midplane or divertor neutral pressures. For our standard shape plasmas at 1 MA, discharges with midplane neutral pressures greater than 0.1 mTorr or with ohmic target densities greater than $1.5-2\times10^{20}\,\mathrm{m}^{-3}$ are predominately EDA. This can be illustrated in Fig. 5(d) where the average triangularity is plotted against midplane neutral pressure. In this plane, regions of predominately EDA and predominately ELM-free can be distinguished. EDA is also correlated with high plasma density, but not as strongly as with neutral pressure.

Edge density profiles measured by reflectometry and electron temperature profiles by electron cyclotron emission (ECE) show widths that can be 1 cm or less, near the limit of the diagnostic resolution.[15] The temperature width does not show any clear trends with those parameters identified as essential for the EDA/ELM-free boundary and ∇Te is found to be roughly constant under a wide range of conditions. To explore the pedestal with greater resolution, an array of soft x-ray detectors was installed. Soft x-ray emission in the edge region originates mainly in recombination continuum from low Z impurities and has very little temperature dependence after accounting for transmission through the 10 μm Beryllium foil filter. The x-ray emissivity is essentially a measure of $n_e n_z$. The soft x-ray array shows the steepest pedestals of any diagnostic, with widths as small as 2 mm in high current ELM-free H modes (Table I).[16] X-ray profiles are much steeper in ELM-free than in EDA H-modes (see Fig. 7). Soft

TABLE I. Comparison of EDA and ELM-free characteristics and a summary of the conditions under which each in predominate.

	ELM-free H mode	EDA H mode
Energy confinement	$H_{89}\sim2.1$	$H_{89}\sim1.9$
Particle confinement	$\tau_1\gg\tau_E$	$\tau_1\sim2-3\times\tau_E$
Edge fluctuations	None observable	Broadband and coherent fluctuations
X-ray pedestals	Narrow 2–6 mm	Wide 6–12 mm
Dependence on q_{95}	More likely when $q_{95}<3.7$	More likely when $q_{95}>3.7$
Dependence of δ	$\delta<0.35$ $\delta>0.55$	moderate plasma shaping $0.35<\delta<0.55$
Dependence on neutrals	Favored at low neutral pressure	Favored at high neutral pressure

x-ray widths also show an inverse dependence on plasma current and a positive correlation with triangularity (Figs. 8 and 9). Parameters which cause the x-ray width to drop are generally the same as those which cause transitions from EDA to ELM-free behavior. Temperature pedestal widths show relatively little dependence on the type of H mode, which may suggest that the EDA regime mainly affects the density pedestal. This would be consistent with the observed weak effect on global energy confinement and the strong effect on particle confinement.

IV. DISCUSSION

Perhaps the most important questions that we wish to answer concern the physical mechanism that leads to EDA behavior and its applicability in reactor regimes. In the EDA regime, the edge pedestal gradients are relaxed by a continuous rather than an intermittent process. Even when small ELMs are seen on top of the EDA as shown in Fig. 2, these do not seem to carry out any significant amount of energy or particles, nor do they diminish the size of the pedestal. In contrast, type I ELMs are believed to be a relaxation oscillation driven by the improved transport in the H-mode barrier and limited by pressure driven[17] or current driven[18] MHD modes. Hegna[19] and Connor[20] have formulated a picture for ELM behavior by calculating stability in the J_a, α

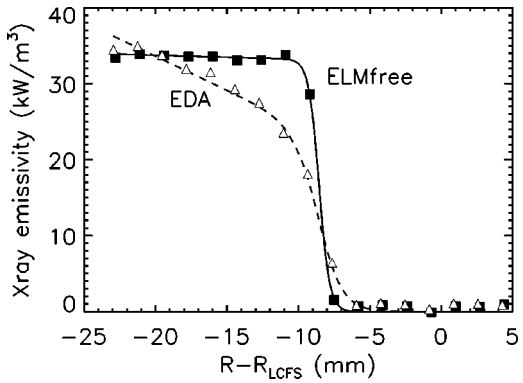

FIG. 7. A comparison between the edge x-ray pedestals in EDA and ELM-free H modes. ELM-free plasmas consistently show much steeper profiles. In this case, the ELM-free pedestal width is at the limit (1–2 mm) of the x-ray diagnostic.

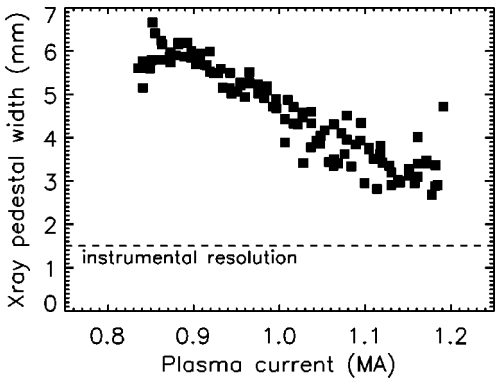

FIG. 8. The x-ray pedestal width during a scan of plasma current at constant field and plasma shape during an EDA H mode. The observed variation, narrow profiles at high current and wide profiles at low current, is consistent with the I_P dependence of the EDA/ELM-free boundary discussed earlier.

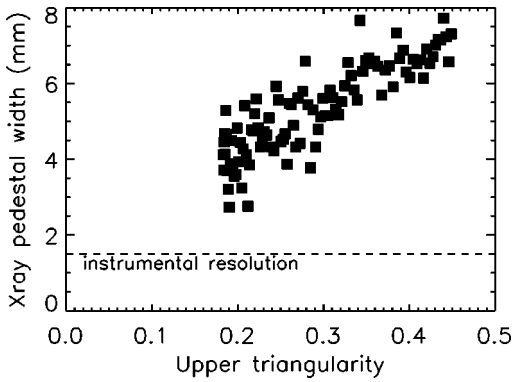

FIG. 9. The x-ray pedestal width during a scan of upper triangularity at constant field and plasma current during an EDA H mode. The observed variation is consistent with the δ dependence of the EDA/ELM-free boundary discussed earlier.

plane (where J_a is the edge current density and α is the normalized edge pressure gradient, $R\beta'$). In this picture, the edge of an H-mode plasma evolves to the pressure driven ballooning limit on a transport time scale, then toward the current driven ''peeling mode'' limit on a current diffusion time scale. The ballooning limit is seen as a ''soft'' limit, where transport is increased but the pedestal remains intact. ELMs are identified with the peeling limit, which is essentially an external kink, and results in destruction of the barrier. (We note that one might expect to see an increase in edge turbulence as an ELM-free discharge approaches its first large ELM; in fact this is not generally observed.) In this picture, one might identify EDA as a manifestation of the ballooning limit. The observed dependence on triangularity and safety factor in the EDA/ELM-free boundary, suggests that MHD stability does play an important role. Superficially, the dependencies are reminiscent of those reported by Miller,[21] where the plasma edge was shown to have the easiest access to second stability at moderate δ and at higher q_{95}. However, to make that connection, we would have to identify EDA as the more MHD stable regime. This view is contradicted by the increased level of turbulence and decreased particle confinement seen in EDA.

The MHD stability of the pedestal is rather difficult to analyze however, depending critically on the local magnitude of edge current density and pressure gradient. Thus individual flux surfaces within the pedestal may be near one of several stability limits. The effects of shaping and safety factor discussed above cannot be explained by a simple S/q^2 analysis (S is the global shear and q is the edge safety factor) which was used to explain the type I ELM boundary in DIII-D.[17] Resolution of these issues must await improved measurements of pedestal profiles planned for future experimental campaigns. The observed effects of neutrals may ultimately be explained within the same model of the peeling mode. We note that high levels of neutrals in the plasma edge can lower the edge temperature through direct cooling (via charge exchange and convective losses) or by weakening the transport barrier via shear flow damping. We have observed slower mode rotation at high neutral densities, which can be interpreted as damping of the underlying perpendicular flows.[14] Regardless of the mechanism, lower edge temperatures are observed at high neutral densities from which we can infer higher collisionalities and smaller edge currents from both the ohmic and bootstrap drives. These effects will tend to keep the plasma edge away from the peeling boundary and thus suppress type I ELMs. Finally we note the possible connection to theories of drift Alfven turbulence. Three dimensional electromagnetic simulations show that plasmas at higher collisionality are subject to turbulence due to the nonlinear evolution of resistive ballooning modes and ion thermal gradient instabilities.[22] It is possible that EDA is a manifestation of this turbulence.

ACKNOWLEDGMENTS

The authors wish to thank the entire Alcator staff for their hard work and dedication in support of these experiments. Work supported by U.S. Department of Energy Contract No. DE-AC02-78ET51013.

[1] G. Mathews and JET team, *Proceedings of the 17th International Fusion Energy Conference, Yokohama, Japan, 1998* (International Atomic Energy Agency, Vienna, 1999).
[2] J. A. Snipes, R. Boivin, C. Fiore *et al.*, *Proceedings of the 24th EPS Conference, Berchtesgaden, European Physical Society* (Petit-Lancy, Switzerland, 1997), Vol. 21A, Part II, p. 565.
[3] M. Greenwald, R. L. Boivin, F. Bombarda *et al.*, Nucl. Fusion **37**, 793 (1997).
[4] H. Zohm, Plasma Phys. Controlled Fusion **38**, 105 (1996).
[5] J. E. Rice, J. L. Terry, J. A. Goetz, Y. Wang, E. S. Marmar, M. Greenwald, I. Hutchinson, Y. Takase, S. Wolfe, H. Ohkawa, and A. Hubbard, Phys. Plasmas **4**, 1605 (1997).
[6] M. Bures, D. J. Campbell, N. Gottardi *et al.*, Nucl. Fusion **32**, 539 (1992).
[7] Y. Kamada, R. Yoshino, Y. Neyatani *et al.*, Plasma Phys. Controlled Fusion **38**, 1387 (1996).
[8] T. Ozeki, M. S. Chu, L. L. Lao *et al.*, Nucl. Fusion **30**, 1425 (1990).
[9] J. A. Snipes, R. Granetz, M. Greenwald *et al.*, Plasma Phys. Controlled Fusion **40**, 765 (1998).
[10] J. G. Cordey and ITER confinement database and modeling working group, Plasma Phys. Controlled Fusion **39**, B115 (1997).
[11] P. Yushmanov, T. Takizuka, K. Riedel, O. Kardaun, J. Cordey, S. Kaye, and D. Post, Nucl. Fusion **30**, 1999 (1990).
[12] P. Stek, Ph.D. thesis, Massachusetts Institute of Technology, 1997.
[13] Y. Lin, J. Irby, P. Stek, I. Hutchinson, J. Snipes, R. Nazikian, and M. McCarthy, Rev. Sci. Instrum. (to be published).
[14] I. H. Hutchinson, R. S. Granetz, A. Hubbard, J. A. Snipes, T. Sunn Ped-

ersen, M. Greenwald, and B. LaBombard, Plasma Phys. Controlled Fusion (to be published).
[15]A. E. Hubbard, R. L. Boivin, R. S. Granetz, M. Greenwald *et al.*, Phys. Plasmas **5**, 1744 (1998).
[16]Granetz, R., Osborne, T., R. L. Boivin, M. Greenwald, R. J. Groebner, A. E. Hubbard, J. H. Irby, L. L. Lao, A. W. Leonard, Y. Lin, R. L. Miller, T. Sunn Pedersen, and G. D. Porter, *Proceedings of the 17th International Fusion Energy Conference, Yokohama, Japan, 1998* (International Atomic Energy Agency, Vienna, 1999).
[17]P. Gohil, M. Ali Mahdavi, L. Lao *et al.*, Phys. Rev. Lett. **61**, 1603 (1988).
[18]J. Manickam, Phys. Fluids B **4**, 1901 (1992).
[19]C. Hegna, J. W. Connor, R. J. Hastie, and H. R. Wilson, Phys. Plasmas **3**, 584 (1996).
[20]J. W. Connor and H. R. Wilson, *Theory of Fusion Plasmas*, edited by J. W. Connor, E. Sindoni, and J. Vaclavik (Editrice Composotiori, Bologna, 1997), p. 441.
[21]R. L. Miller, Y. R. Lin-Liu, T. H. Osborne, and T. S. Taylor, Phys. Plasmas **4**, 1062 (1996).
[22]B. N. Rogers and J. F. Drake, Phys. Rev. Lett. **79**, 229 (1997).